Intracellular pH Transients in Squid Giant Axons Caused by CO_2, NH_3, and Metabolic Inhibitors

WALTER F. BORON and PAUL DE WEER

From the Department of Physiology and Biophysics, Washington University School of Medicine, St. Louis, Missouri 63110

ABSTRACT The intracellular pH (pH_i) of squid giant axons has been measured using glass pH microelectrodes. Resting pH_i in artificial seawater (ASW) (pH 7.6–7.8) at 23°C was 7.32 ± 0.02 (7.28 if corrected for liquid junction potential). Exposure of the axon to 5% CO_2 at constant external pH caused a sharp decrease in pH_i, while the subsequent removal of the gas caused pH_i to overshoot its initial value. If the exposure to CO_2 was prolonged, two additional effects were noted: (*a*) during the exposure, the rapid initial fall in pH_i was followed by a slow rise, and (*b*) after the exposure, the overshoot was greatly exaggerated. Application of external NH_4Cl caused pH_i to rise sharply; return to normal ASW caused pH_i to return to a value below its initial one. If the exposure to NH_4Cl was prolonged, two additional effects were noted: (*a*) during the exposure, the rapid initial rise in pH_i was followed by a slow fall, and (*b*) after the exposure, the undershoot was greatly exaggerated. Exposure to several weak acid metabolic inhibitors caused a fall in pH_i whose reversibility depended upon length of exposure. Inverting the electrochemical gradient for H^+ with 100 mM K-ASW had no effect on pH_i changes resulting from short-term exposure to azide. A mathematical model explains the pH_i changes caused by NH_4Cl on the basis of passive movements of both NH_3 and NH_4^+. The simultaneous passive movements of CO_2 and HCO_3^- cannot explain the results of the CO_2 experiments; these data require the postulation of an active proton extrusion and/or sequestration mechanism.

INTRODUCTION

Since the pioneering work of Caldwell (1954), several workers (Caldwell, 1958; Spyropoulos, 1960; Kostyuk et al., 1969; Carter et al., 1967; McLaughlin and Hinke, 1968; Paillard, 1972; Bicher and Ohki, 1972; and Thomas, 1974 *a, b*) have studied the intracellular pH (pH_i) of excitable tissues by means of microelectrodes. They have established normal values and examined factors responsible for pH_i alteration. With the exception of Carter et al. (1967), all the above investigators found that the intracellular proton activity is substantially lower than that predicted by a passive Donnan distribution. In studies on axons of the squid *Loligo forbesi,* Caldwell (1958) reported that pH_i was normally near 7. For axons of *Loligo pealei,* Spyropoulos (1960) found that pH_i was approximately 7.35, while Bicher and Ohki reported a value of 7. Although pH_i is relatively insensitive to experimental manipulation, increases in p_{CO_2} cause a rapid acidification in squid axon (Caldwell, 1958). Similarly, Thomas (1974 *a*), working with snail neurons, found that NH_3 and CO_2 cause rapid and large pH_i changes,

whereas anoxia, Na azide, and 2,4-dinitrophenol (DNP) produce smaller alterations (Thomas, 1974 *a*).

We now report a study of pH_i in squid giant axons. Special attention was given to the calibration of pH-sensitive, glass microelectrodes. The pH-sensitive area of these electrodes was at least two orders of magnitude smaller than that of those previously used in squid axons (Caldwell, 1958; Spyropoulos, 1960). A series of steady-state measurements were made in normal seawater previous to further manipulations. These experiments establish that the intracellular pH_i of the giant axon of *Loligo pealei* in artificial seawater (ASW) is near 7.3.

In addition, we examined the kinetics of pH_i transients created by sudden changes in external conditions, such as addition or removal of CO_2, NH_4Cl, NaCN, DNP, and azide. The temporal pH_i changes observed in these weak electrolyte experiments are complex, and are not all intuitively interpretable. It has long been known that the rate of permeation and distribution of weak acids and bases across cell membranes is dependent on extra- and intracellular pH, and also that exposure of cells to solutions containing certain weak acids or bases could lead to rapid intracellular pH changes. Jacobs (1940) clearly identified the fundamental principles governing these phenomena. On the assumption that only the *uncharged* partner of the conjugate pair is permeant, he derived an equation for the *steady-state* transmembrane distribution of a weak acid or base as a function of its dissociation constant and both intra- and extracellular pH. In their study of the excretion of ammonia and other weak bases by the kidney, Orloff and Berliner (1956) employed an equilibrium treatment which included a finite permeability to the charged partner of the conjugate pair. However, their approach required that there be no electrical potential difference across the epithelium. Finally, a rigorous steady-state analysis of the transmembrane distribution of a weak acid was provided by Roos (1965, 1971, 1975) who took into account membrane potential as well as the permeability to both the charged and uncharged forms. The extreme case of exclusive permeability to the neutral species reduces the equation of Roos to that of Jacobs (1940), whereas exclusive permeability to the charged species (provided $pH \gg pK_a'$) simplifies Roos' equation to that of Donnan (1924).

We have developed a mathematical model which describes the kinetics of the movement of both partners of a conjugate pair of a weak electrolyte across the cell membrane and the attendant changes in pH_i. This model satisfactorily explains the transients observed in our experiments and provides a means of estimating several system parameters. Certain aspects of the experiments with CO_2 require the additional postulation of an active proton extrusion and/or consumption mechanism responsive to proton loads. As expected, our equations, when constrained to the conditions of steady state, reduce to those of Roos (1965, 1975). Part of this work has been communicated in preliminary form (Boron and De Weer, 1975).

METHODS

General

The experiments were performed at the Marine Biological Laboratory in Woods Hole, Mass., during the months of June 1974 and May 1975. Giant axons (average diameter, 540

μm) from the hindmost stellar nerve of live specimens of the squid *Loligo pealei*, were cleaned and both ends were tied to glass cannulae. The axons were incubated in a horizontal dialysis chamber (Brinley and Mullins, 1967) kept at 23°C. The chamber (vol, 0.15 ml) was continuously perfused with seawater at a rate of 2 ml/min.

Solutions

ASW, used in all experiments, had the following composition (in mM): 425 NaCl, 10 KCl, 25 $MgCl_2$, 10 $CaCl_2$, 25 $MgSO_4$. Tris-HEPES (5 mM) buffered all solutions (including CO_2-containing media) to pH 7.6–7.8. When CO_2 was used, we equilibrated solutions in the supply reservoir with 5% CO_2–95% O_2 for at least 1 h before and continuing throughout the experiment; 50 mM $NaHCO_3$ was substituted for 50 mM NaCl. In the CO_2 seawater, $CaCl_2$ was added just before the experiment began, and some precipitate was noted by the experiment's end. Either 10, 9, or 3 mM NH_4Cl, nominally 2 mM NaCN, 1 mM 2,4-dinitrophenol, and 3 mM NaN_3 were added directly to normal seawater. In 100 K-ASW, 90 mM KCl was substituted for NaCl, although in K-free or 1 mM K-ASW, no substitution was made for the absent KCl.

Electrodes

We inserted membrane and pH electrodes through cannulae at opposite ends of the axon. The pH electrodes were constructed of Corning 0150 pH-sensitive glass and Corning 0120 lead glass (Corning Glass Works, Corning, N.Y.) according to the design of Hinke (1967). They had exposed, pH-sensitive glass tips of approximately 10–15-μm diameter × 50-μm length, and lead glass shanks which maintained a diameter of less than 100 μm for at least the terminal 3 cm. The drift of these electrodes was less than 1 mV over 24 h; they responded to changes in pH within a few seconds, were linear over the pH range 5.87–7.89, and had an average slope of 56.9 mV/pH.

The borosilicate glass membrane potential electrodes had dimensions similar to those of the pH electrodes, tip potentials of approximately −0.5 mV, and resistances of 0.8 to 1.1 MΩ. Membrane potentials recorded from these electrodes were very stable, and reproducibility was routinely better than ±0.3 mV when the membrane potential was changed with pulses of K-free ASW. The external electrodes were similar to the membrane potential electrodes.

pH Standards

From theoretical considerations, Bates (1973) has stated that primary pH standards should be dilute, aqueous solutions of simple solutes in the intermediate pH range (2.5–11.5). In making test measurements the composition of the unknown should match the standard's as closely as possible, a condition which is not met when measuring the pH of a concentrated and ionically undefined intracellular medium after standardization with a primary standard. Thus, the inaccuracy of pH_i measurements with respect to primary standards is of unknown magnitude. Another major difficulty is the drift in electrode output often seen when the solution in which a pH electrode is immersed is suddenly changed to one with a very different ionic strength. This latter problem has been overcome after a suggestion of Bates (personal communication). We have prepared a series of six secondary buffers using different ratios of primary to secondary potassium phosphates (at a constant total phosphate concentration of 50 mM) plus enough potassium chloride to make the total ionic strength 0.600 M, similar to the buffers of Valensi and Maronny (Bates, 1973). Using primary standards of the National Bureau of Standards of the United States (NBS) (0.05 m KH phthalate and 0.025 m KH_2PO_4/0.025 m K_2HPO_4, obtained from Harleco, Philadelphia, Pa.) to calibrate a standard macro combi-

nation pH electrode and an Instrumentation Laboratory, Inc., Lexington, Mass., model 245 pH meter, we measured the pH of each of the six buffers at several temperatures. The pH measured in each of the new buffers was then assigned to that solution. It was not necessary to oven-dry the salts of the high ionic strength buffers before weighing, since their assigned pH values were determined solely by comparison with NBS standards. We used these high ionic strength buffers to calibrate all intracellular pH electrodes. It should be pointed out that the use of these secondary standards does not increase the accuracy of our measurements with respect to primary NBS standards; the advantage is that drift is minimized.

Electrical Connections

We coupled the 3 M KCl membrane and external reference electrodes (via calomel half cells) and the pH_i electrode to individual 311K electrometers (Analog Devices, Inc., Norwood, Mass.) in the single-ended configuration (input impedance, 10^{14} Ω). A gold wire in the chamber was connected to the system's ground. Operational amplifiers (Burr-Brown Research Corp., Tucson, Ariz., 3500 *A* and Analog Devices *118A*) electronically subtracted the signals of the membrane electrode from that of the pH_i electrode to produce the potential due to intracellular pH (V_{pH}), and the signal of the external reference electrode from that of the membrane electrode to yield the membrane potential (V_m). We could display each potential on a digital voltmeter (read to the nearest millivolt) and record them on a strip chart recorder. A filter with a time constant of 9 s was used at the input of each channel of the strip chart recorder.

Calculations

The intracellular pH was calculated using the following equation:

$$pH_i = pH_s - \frac{V_s - V_{pH}}{S},$$

where pH_s is the pH of one of the standards, V_s the potential recorded in that standard, V_{pH} the net potential due to pH_i, and S the slope (millivolts per pH) between two or more standards. The pH_i values given in the figures in this paper do not include corrections for liquid junction potential.

RESULTS

Normal Intracellular pH

For 22 axons in normal ASW of pH 7.61–7.80, the uncorrected pH_i was 7.32 ± 0.013 (SEM) and the membrane potential −56.5 ± 0.7 mV. If the junction potential correction of Cole and Moore (1960) is made for our data, the mean pH_i would drop to 7.28. This pH_i is significantly higher than pH 6.73, predicted from Donnan theory using V_m = −56.5 mV. Spyropoulos (1960) found a value for pH_i of 7.40 ± 0.10 before, or 7.35 ± 0.10 after applying a correction for liquid junction potential. Caldwell (1958) reports that the normal pH_i of *Loligo forbesi* is near 7, although examination of his Fig. 17 yields an average normal pH_i of near 7.10. It is not clear whether Caldwell applied any correction for junction potentials occurring with 3 M KCl electrodes. Bicher and Ohki's data (1972) yielded an intracellular pH of 7.0. The nonlinearity of their antimony

electrodes in the physiological range and the very large uncertainty (±0.2 pH units) in their measurements make the interpretation of their results difficult.

Carbon Dioxide Experiments

In his experiments with squid axons, Caldwell (1958) found that only application of CO_2 ($pK_a' \simeq 6.00$) produced rapid and large changes in pH_i. He did not examine the reversibility of the CO_2 effect. As illustrated in Fig. 1 A, we similarly found that exposure to 5% CO_2 produced a sharp fall in pH_i, averaging 0.38 ± 0.05 (SEM) pH units ($n = 8$). After termination of short-duration exposures to CO_2 (approximately 5 min), pH_i promptly returned to a value which was consistently higher than the initial one. In the experiment of Fig. 1 A this overshoot amounted to about 0.04 pH units.

In three experiments, we maintained exposure of the axon to CO_2 for as long as 80 min, as illustrated in Fig. 1 B. As usual, pH_i initially fell sharply. However, after about 5 min pH_i began to slowly climb at an average rate of 0.10 ± 0.04 pH units/h (we shall call such a period of relatively slow pH_i change a "plateau phase"). When we removed the CO_2-ASW, pH_i rapidly rose beyond the axon's initial pH_i to a value considerably more alkaline. The size of the overshoot was positively related to the magnitude of the pH_i rise during the plateau phase. We observed only small changes in membrane potential (Fig. 1 A and B) during and after exposures to CO_2.

There is little doubt that in these experiments, the passive entry of CO_2 and its subsequent hydration and dissociation to form H^+ and HCO_3^- causes the initial decline in pH_i (Jacobs, 1940). During the first few instants of exposure to CO_2 an inward gradient for HCO_3^- also exists, though the influx of this ion (which would blunt the acidification produced by CO_2 influx) may be small due to either a low permeability and/or the effects of membrane potential. Soon thereafter, however, the concentration of intracellular CO_2 approaches that of external CO_2. If the pK for CO_2 is the same on either side of the membrane, the following identities hold: $[H^+]_i[HCO_3^-]_i = K_a'[CO_2]_i = K_a'[CO_2]_o = [H^+]_o[HCO_3^-]_o$, and therefore $[HCO_3^-]_i$ reaches levels high enough to make the equilibrium potentials for H^+ and HCO_3^- equal. Its electrochemical gradient having now been reversed, HCO_3^- would tend to leave the cell. This would result in a reduction of $[CO_2]_i$, thus maintaining an inward gradient for CO_2 (see Fig. 1 C). These simultaneous, passive fluxes of HCO_3^- and CO_2 would then be expected to lead to a further *acidification* during the plateau phase, yet, an *alkaline* drift was actually observed. This alkaline drift can only be explained by outward H^+ pumping (or its formal equivalent: pumping of HCO_3^- or OH^- in the opposite direction), or, possibly, by an intracellular proton sequestration mechanism. Furthermore, this alkaline drift indicates that the rate of proton pumping exceeds any proton accumulation due to passive shuttling by the CO_2/HCO_3^- couple.

Upon removal of external CO_2, intracellular CO_2 will passively diffuse outward whereas most intracellular HCO_3^- will combine with H^+ and likewise leave as CO_2, thereby nullifying nearly the entire intracellular proton load brought

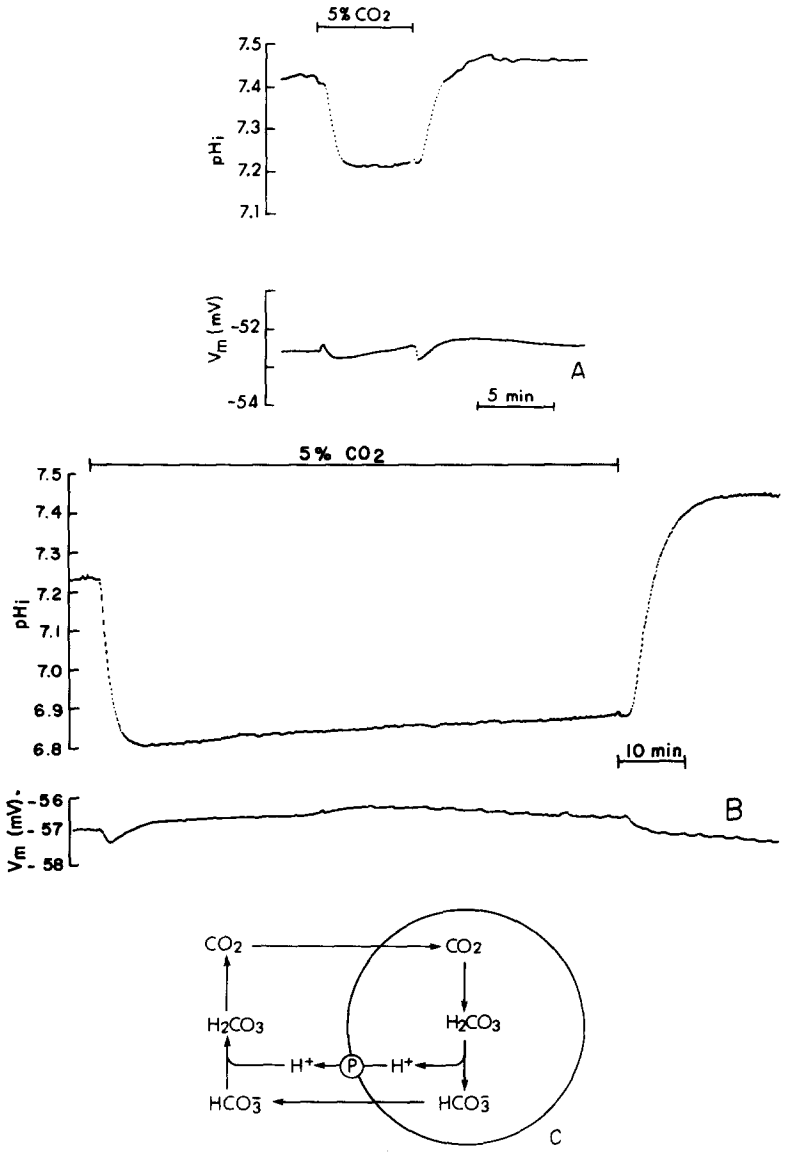

FIGURE 1. (A) Effect of short-term CO_2 exposure on pH_i and membrane potential. During the indicated time the axon was exposed to 5% CO_2 at constant pH_o (7.70). Note the slight overshoot of pH_i upon return to the control ASW. All records have been traced by an artist from original copies. The broken lines which appear during periods of rapid voltage changes are a consequence of the recording pen's alternately tracing the pH_i and V_m curves. (B) Effect of long-term CO_2 exposure on pH_i and membrane potential. The conditions were similar to those in Fig. 1 A except for the longer exposure to 5% CO_2. Note the slow alkalinization during the plateau phase and the exaggerated overshoot upon return to ASW. (C) Inward shuttling of protons by the CO_2/HCO_3^- couple during the plateau

about by CO_2 entry. However, since additional protons had been pumped out during the CO_2 exposure, pH_i, upon removal of external CO_2, should be higher than its initial value. The magnitude of this overshoot should be a function of the algebraic sum of protons pumped from the axon and those passively shuttled in the opposite direction. It might be pointed out that any passive exit of HCO_3^- during the CO_2 efflux phase would only serve to blunt this overshoot, and that the amount of HCO_3^- exiting after the removal of CO_2 would be expected to be much greater than the amount which entered during the first moments of CO_2 exposure, due to the effect of membrane potential.

The small overshoots seen after CO_2 exposures of short duration (Fig. 1 A) were most likely caused by the proportionately smaller amounts of H^+ pumped. It is interesting to note that in one experiment several successive short CO_2 exposures had the effect of progressively increasing the value to which pH_i rebounded after CO_2 removal. This is to be expected, since the H^+ pumping which occurs during the short CO_2 exposures is cumulative in its effects on pH_i. A mathematical formulation of these events has successfully mimicked the observed changes in pH_i seen with CO_2 application and removal (see Appendix).

Ammonia Experiments

Exposure of axons to 9–10 mM NH_4^+ ($pK_a' \simeq 9.5$) at pH 7.7 resulted in a rapid increase in pH_i by 0.51 ± 0.02 pH units ($n = 8$), as illustrated in Fig. 2 A. A smaller increase (0.34 pH) was noted in one axon where 3 mM NH_4^+ was used. Return to ASW within 8–25 min caused pH_i to drop to a value 0.07 ± 0.02 ($n = 4$) below the starting point. These undershoots were observed after a period of exposure to NH_4^+ so brief that pH_i was still increasing with time when the NH_4^+ was removed. During the period of exposure to NH_4^+, the membrane potential depolarized by 2.4 ± 0.1 mV ($n = 8$) and, upon removal of NH_4^+, returned to its initial level within ± 0.1 mV. It is interesting to note that a change from 10 K to 20 K-ASW caused a similar degree of depolarization, 2.7 ± 0.1 mV ($n = 4$).

The initial alkalinization seen during the first moments of exposure to NH_4^+ is presumably caused by the rapid, passive entry of NH_3 and its subsequent hydration to form NH_4^+ and OH^- (Jacobs, 1940). If the membrane exhibits a finite permeability to NH_4^+ as well, this would result in an influx of this ion early during the exposure to NH_4Cl. Such an influx would temper the alkalinization due to NH_3 influx, since a small fraction of these ions dissociate to form protons and NH_3. Thus, even as pH_i is rising, some H^+ would be carried into the axon by the incoming NH_4^+. Removal of external NH_4^+, at this point, will result in an exit of NH_3 and NH_4^+. However, since the driving force for net efflux of NH_4^+ is less than for the previous influx of these ions (due to the effect of membrane potential), the fiber should lose fewer of these proton carriers than it has gained. For this reason it is expected that after withdrawal of NH_4Cl from the medium, pH_i will be lower than before exposure, as can be seen in Fig. 2 A.

---

phase. Any efflux of HCO_3^- down its electrochemical gradient would maintain an intracellular sink for CO_2. The inward proton shuttling produced by such a mechanism during the plateau phase of Fig. 1 B would have to be more than offset by H^+ extrusion to account for the observed slow alkalinization.

If exposure to NH_4^+ is prolonged (Fig. 2 B), the rate of NH_3 influx will decline and eventually vanish. At this point (assuming pK_a' for ammonium to be identical on both sides of the membrane), the following identities will hold: $[H^+]_i/[NH_4^+]_i = K_a'/[NH_3]_i = K_a'[NH_3]_o = [H^+]_o/[NH_4^+]_o$. In other words, the

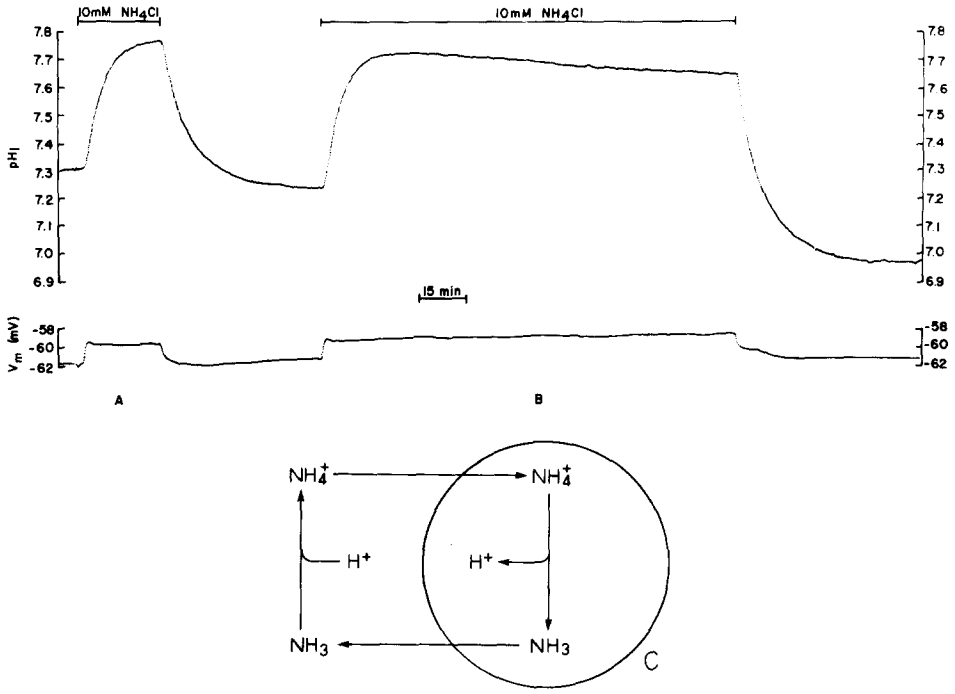

FIGURE 2. (A) Effect of short-term NH_4Cl exposure on pH_i and membrane potential. During the time indicated, the ASW bathing the axon contained 10 mM NH_4Cl at constant pH_o (7.70). Note the undershoot of pH_i upon return to control ASW. (B) Effect of long-term NH_4Cl exposure on pH_i and membrane potential. During the time indicated, the axon was exposed to ASW containing 10 mM NH_4Cl. Note that the prolonged NH_4Cl treatment leads to a slow acidification following the initial decrease in pH_i. (C) Suggested mechanism for inward shuttling of protons by the NH_3/NH_4^+ couple during the plateau phase of Fig. 2 B. The continuing influx of NH_4^+ down its electrochemical gradient maintains an intracellular source of NH_3. The net proton influx produced by this shuttling mechanism is presumably responsible for the slow acidification observed during the plateau phase of Fig. 2 B. Although the electrochemical gradient for protons is inward, the absolute flux of H^+ per se is expected to be very small due to the low concentration of this ion.

equilibrium potential for NH_4^+ will be identical to that for H^+ (i.e., less negative then V_m). Consequently, since its electrochemical gradient remains inward, NH_4^+ continues to enter. Moreover, since a fraction of these ions dissociate upon entry to form NH_3 and H^+, an outward gradient for NH_3 will be created. The net effect of these two simultaneous fluxes is the inward shuttling of protons (see Fig. 2 C), which should lead to a gradual acidification of the cell. This is indeed

what we observed during prolonged exposures to NH_4^+ (see the plateau phase of Fig. 2 B): pH_i declined at an average rate of 0.08 ± 0.02 pH/h (n = 4). After return to ASW the undershoot of pH_i was greatly exaggerated. A mathematical statement of these events is given in the Appendix.

The triphasic time-course of V_m during the first moments of exposure to NH_4Cl was consistently observed in other experiments, and may have several explanations. The rapid initial depolarization plainly results from the K^+-like effect of external NH_4^+. The second (hyperpolarizing) phase may be due to the intracellular accumulation of NH_4^+, the osmotic exit of water, or to a combination of both. A third (depolarization) phase would be expected if a significant loss of K^+ occurs or if NH_4^+ accumulation lags appreciably behind the water movement.

Cyanide Experiments

The exposure of axons to nominally 2 mM NaCN at pH 7.70, after a 5-min delay, caused a slow fall in pH_i which continued for 30–60 min (see Fig. 3 A). The total decrease in pH_i averaged 0.27 ± 0.02 pH units in four experiments. In each of these experiments, the membrane voltage showed a slight depolarization, followed by a marked hyperpolarization of as much as 7 mV or more after 1 h. The existence of these peculiar effects of CN on membrane potential has been noted by De Weer and Geduldig (1975) and is the subject of continuing investigation. Removal of external CN led to a partial recovery of pH_i, which after approximately 5 min averaged 0.12 ± 0.01 pH units. The membrane potential responded by depolarizing to a value near its initial level.

Since the pK_a' for HCN (approx. 10) is so much larger than pH_i, the entry of HCN produces very few protons by dissociating to form $CN^- + H^+$. Thus, a fairly rapid intracellular acidification, analogous to that seen with the onset of CO_2 exposure, is not to be expected with HCN. Furthermore, because $[CN^-]_i$ is so low (we calculate ~ 2 μM), the permeability of the membrane to CN^- would have to be exceedingly large to explain the long-term intracellular acidification on the basis of the shuttling hypothesis. It is more likely that the acidification seen is due to some metabolic inhibitory effect of HCN, and the resultant buildup of intracellular acids.

DNP and Azide Experiments

Fig. 3 B and C show the effects of long-term exposure of an axon to DNP and azide, respectively. Each type of experiment was performed on three axons. Mitchell (1961) has interpreted the ability of DNP ($pK_a' \simeq 4.0$) to uncouple oxidative phosphorylation on the basis of its acting as a proton shuttler across mitochondrial inner membrane. Thus, exposure to DNP may decrease pH_i in at least three ways: (*a*) by penetrating the plasma membrane as DNP and dissociating to form H^+ and dinitrophenoxide ions (DNP^-), (*b*) by shuttling H^+ across the plasma membrane via the influx of DNP and the efflux of DNP^-, and (c) by causing a buildup of metabolic acids due to its effect on mitochondria. It is very difficult to distinguish among the three alternatives experimentally. It should be pointed out that the initial fall in pH_i started shortly after exposure to DNP, and

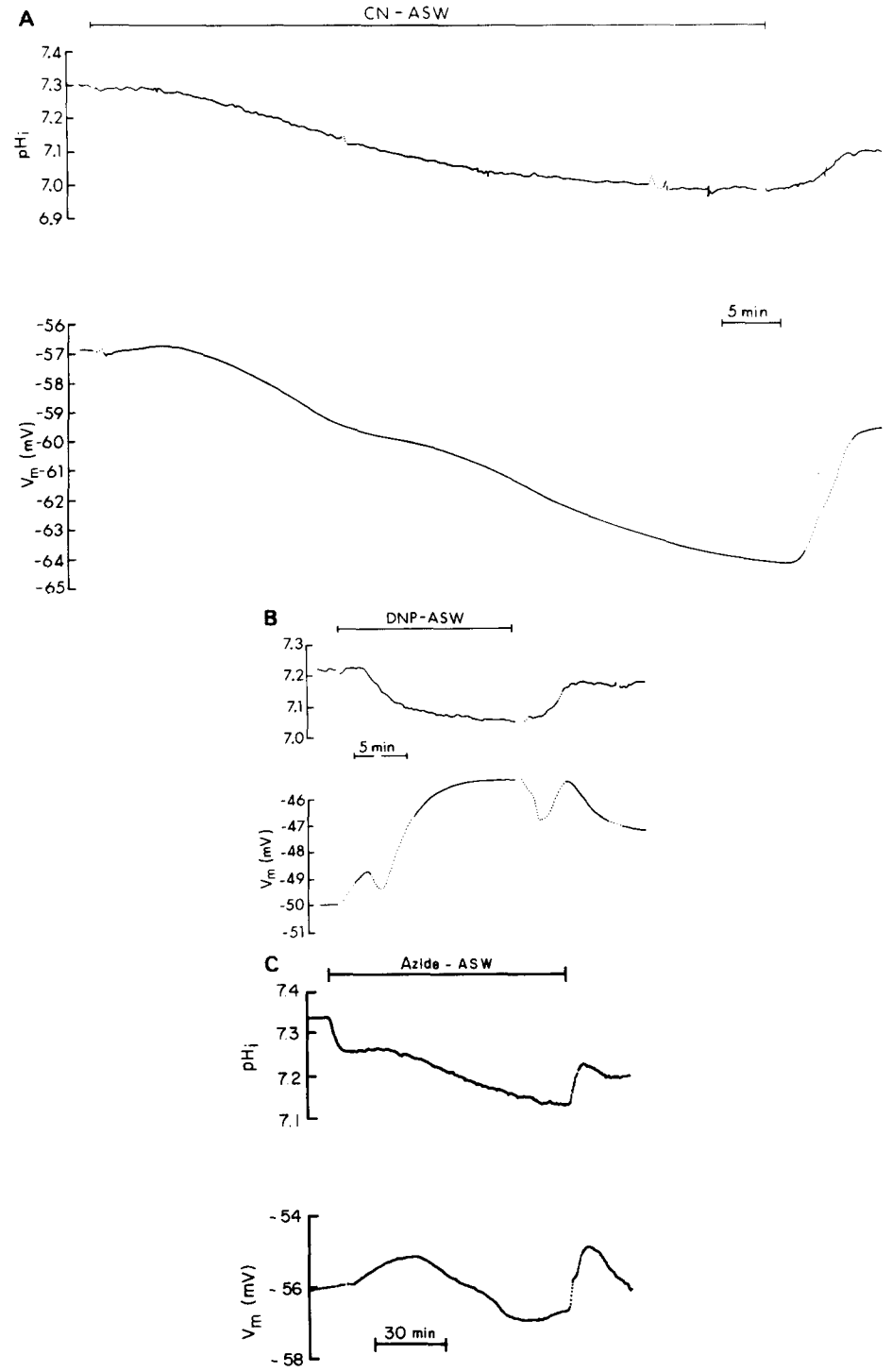
A
CN - ASW
7.4
7.3
7.2
7.1
7.0
6.9
pHi
5 min
-56
-57
-58
-59
-60
-61
-62
-63
-64
-65
Vm (mV)
B
DNP-ASW
7.3
7.2
7.1
7.0
5 min
-46
-47
-48
-49
-50
-51
Vm (mV)
C
Azide - ASW
7.4
7.3
7.2
7.1
pHi
-54
-56
-58
Vm (mV)
30 min

that its initial rate of fall was more than five times greater than that produced by CN. We have no explanation for the changes in V_m.

Azide ($pK_a' \simeq 4.7$), which also uncouples oxidative phosphorylation (Mitchell, 1961), produces an abrupt fall in pH_i, whose reversibility depends upon the length of exposure (see Figs. 3 C and 4). This sequence of pH_i changes is qualitatively similar to that seen with CO_2; the initial fall in pH_i is probably caused by an influx of HN_3 which then dissociates to form N_3^- and H^+ intracellularly. The slow fall in pH_i seen during chronic exposure may be due to proton shuttling. Accumulation of metabolic acid and the reduced activity of the proton pump cannot be ruled out.

It should be noted that azide pulses had identical effects on pH_i in the presence of either 100 or 10 mM K-ASW (two experiments) even though the directions of the electrochemical gradients for H^+ in the two cases are opposite (see Fig. 4). If poisoning of a proton pump in the face of a continuing proton influx were responsible for the acidification produced by azide in 10 mM K^+, as has been suggested as a possibility in the snail neuron by Thomas (1974 *a*), then reversing the H^+ electrochemical gradient should produce alkalinization, even in the absence of pumping; this is clearly not the case. It therefore seems more probable that the immediate fall in pH_i observed under both conditions is due to the influx and subsequent dissociation of the acid HN_3.

DISCUSSION

Normal pH_i

Because of the wide discrepancy among published values for pH_i in squid giant axons, a major aim of this work was to attempt to measure pH_i in carefully prepared axons using glass pH microelectrodes characterized by their high stability and small size. Apart from its intrinsic interest, a precise knowledge of pH_i is important in a number of calculations (for instance, those involving the stability constants of such metal-ligand complexes as Mg-nucleotide and Mg- or Ca-EGTA, some of which are quite pH sensitive). "Normal pH_i" values must be interpreted with caution. Ours were determined in nominally CO_2-free ASW. When these same axons were bathed in natural seawater (NSW), however, the pH_i values often were 0.02–0.04 pH units lower (presumably because NSW contains a significant amount of HCO_3^-). Furthermore, the in vivo environment

FIGURE 3. (A) Effect of long-term exposure to CN on pH_i and membrane potential. During the indicated time, the axon was exposed to nominally 2 mM NaCN at constant pH_o (7.70). Note the 5-min delay between the introduction of CN^- and the initial fall in pH_i. See text for additional information. (B) Effect of long-term exposure to DNP on pH_i and membrane potential. During the indicated time the axon was exposed to ASW containing 1 mM DNP at constant pH_o (7.70). Note that the onset of the initial acidification is more rapid and that the initial rate of pH_i fall is much greater than in the case of CN. This axon was previously exposed to DNP for about 5 min. (C) Effect of long-term exposure to azide on pH_i and membrane potential. The axon was exposed to ASW containing 3 mM NaN_3 at constant pH_o (7.70) during the indicated time. Note the very rapid rate of initial acidification.

of these axons is probably very different from ASW. If the p_{CO_2} of the extracellular fluid, for instance, is appreciable, transferring the axons to CO_2-free ASW will cause a rapid rise in pH_i, the size of which is a function of the squid's normal p_{CO_2}. Furthermore, it has been clearly documented (Howell et al., 1970) for several poikilotherms that blood pH rises as temperature decreases. And Reeves (1972), using the DMO method to estimate pH_i in frog muscle, has found that

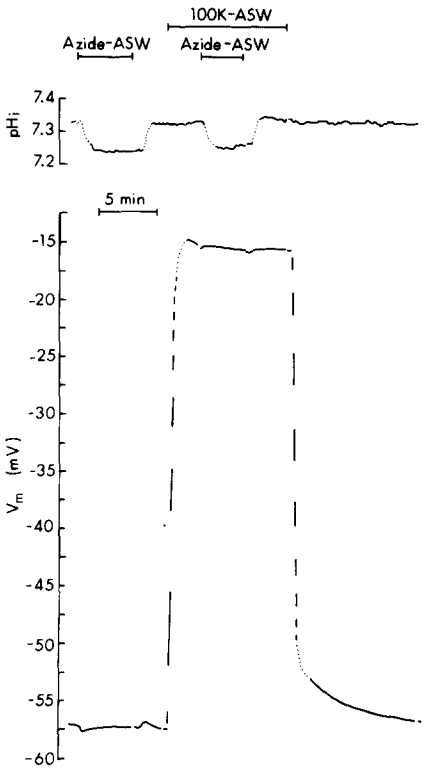

FIGURE 4. Effect of short-term exposure to azide on the pH_i of normal and depolarized squid axons. The axon was briefly exposed to 3 mM NaN_3 before and during membrane depolarization with 100 mM K-ASW. Note that pH_i changes are virtually identical and independent of the direction of the H^+ gradient. The axon had previously received an identical set of azide pulses.

pH_i also is inversely related to acclimated temperature.

For these reasons one must be careful in comparing values for pH_i. Neither Caldwell (1958) nor Spyropoulos (1960) report the composition of their "normal" seawaters or clearly state the temperatures at which their experiments were performed. Our data ($pH_i \simeq 7.3$) agree more closely with those of Spyropoulos, but would not be inconsistent with Caldwell's results if his seawater contained significant amounts of bicarbonate, or if his axons were incubated at a temperature substantially higher than 23°C.

Experiments with CO_2

Our experiments on squid axons exposed to CO_2 and NH_4^+ have confirmed and extended several of the findings of Thomas (1974 *a, b*) who worked with snail neurons. This agreement is significant in view of the differences in species and the style of pH electrode used.

In order to achieve a quantitative understanding of the events underlying the changes in pH_i which occur during and after exposure to CO_2, NH_4Cl, and other weak acids and bases, we have developed a mathematical model (see Appendix for derivation and examples) which has proven a useful tool, not only in the interpretation of our data, but also, in predicting possible events that have thus far not been tested. The model takes into account the simultaneous passive fluxes across the plasma membrane of both the protonated and unprotonated forms of a weak acid or base. Several physicochemical parameters, including the dissociation constant of the weak electrolyte, the permeability of the membrane to both members of the conjugate pair, intracellular buffering power, and membrane potential, are used in calculating the net fluxes of both forms of the weak electrolyte and their effect on pH_i as a function of time. Data which cannot be reconciled with the model, after reasonable manipulation of the system parameters, constitute arguments in favor of some additional process, such as intracellular acid generation or consumption, or changes in the rate of proton extrusion. The model is readily expanded to include a proton pump with arbitrarily defined parameters.

In applying this model to the pH_i changes obtained with exposure to CO_2, we found several aspects of the time-course of pH_i which necessitate the introduction of such additional processes. We refer to the overshoot seen after removal of CO_2 (see Fig. 1 A) and also to the slow increase in pH_i observed during prolonged CO_2 exposure (see Fig. 1 B). As to the rebound upon CO_2 removal, if no pumping mechanism were present, pH_i would return to a value equal to or (if H^+ is shuttled by the CO_2/HCO_3^- couple) less than the initial pH_i. Yet, we consistently found overshoots. As to the pH_i time-course during prolonged exposure to CO_2, in the absence of proton pumping the initial acidification should be followed by a plateau phase which is flat or (if a finite permeability of the membrane to HCO_3^- is assumed, allowing proton shuttling) sloping downwards. Yet, the observed slope was upward. An active proton extrusion mechanism will acount for both anomalies. It is obvious that the proton pumping rate must be high enough not only to produce alkalinization at the observed rate, but also to compensate for any acidification resulting from proton shuttling by the CO_2/HCO_3^- couple. However, numerical solution of the differential equations describing our model (see Appendix) shows that with a bicarbonate permeability similar to that for chloride (approximately 10^{-7} cm/s; calculated from the data of Caldwell and Keynes, 1960), the expected acidification due to proton shuttling will not exceed 0.01 pH/h of exposure to CO_2. An intuitive grasp for the effect of this proton pumping on pH_i may be gained by examining a $[HCO_3^-]$ vs. pH diagram with various CO_2 isopleths. Fig. 5 A has been constructed for squid axoplasm using the data of Harned and Davis (1943) and Harned and Bonner

(1945) for the solubility and first pK_a' of CO_2 in solutions of 0.5 M NaCl. At the start of an experiment p_{CO_2} is very low, and pH_i is described by point A. Introduction of 5% CO_2 (37 mm Hg) raises intracellular p_{CO_2} to nearly the same level and causes a shift in pH_i along the line AB (the slope, which is an expression of the buffering power, is selected to fit the data) to point B. If, at constant p_{CO_2}, protons are pumped out of the cell, pH_i moves along the 5% CO_2

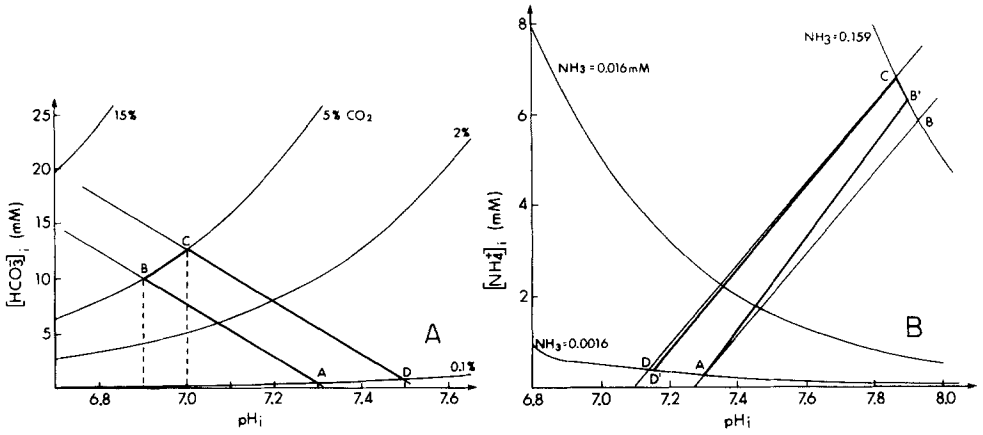

FIGURE 5. (A) Plot of intracellular bicarbonate concentration vs. pH_i at various concentrations of CO_2. The dependence of $[HCO_3^-]_i$ upon pH_i at constant CO_2 has been calculated from the Henderson-Hasselbalch relationship for a variety of CO_2 levels (0.1, 2, 5, and 15% CO_2). The value for buffering power, assumed to be constant (β = −25 mM), was chosen because it gave the best fit. In a system containing CO_2/HCO_3^- in addition to other buffers, the buffering power of these other buffers is given by $\beta = \Delta[HCO_3^-]_i/\Delta pH_i$. Values for pK_a' (6.00) and the solubility of CO_2 (0.0346 mM/mm Hg) in 0.5 M NaCl at 20°C have been taken from the data of Harned and Davis (1943) and Harned and Bonner (1945), respectively. Boldface lines represent the path the system follows in the course of a typical CO_2 experiment. See text for detailed description. (B) Plot of intracellular ammonium concentration vs. pH_i at various concentrations of NH_3. The Henderson-Hasselbalch equation has been used to calculate $[NH_4^+]_i$ as a function of pH_i at constant intracellular NH_3, using pK_a' = 9.5. The three "constant NH_3" curves represent NH_3 concentrations of 0.0016, 0.016, and 0.159 mM. The slope of the lines AB and DC is determined by the intracellular buffering power, β; β = −9 mM fit the data best. In a buffering system which includes NH_3/NH_4^+ in addition to other buffers, the buffering power of these other buffers is described by $\beta = -\Delta[NH_4^+]_i/\Delta pH_i$. See text for additional description.

isopleth to point C. Upon removal of CO_2, pH_i returns to point D, where pH_i is now greater than the initial pH_i. Because of the differing slopes among the CO_2 isopleths, [pH(C) − pH(B)] < [pH(D) − pH(A)]. Inspection of the diagram also illustrates that upon return to the original low p_{CO_2} level, virtually no HCO_3^- remains inside the cell. It is instructive to note two predictions of the model regarding chronic CO_2 exposure: (*a*) pH_i in the plateau phase should progressively increase (because of continual proton extrusion); (*b*) subsequent removal

of CO_2 should produce an overshoot which is greater, the longer the preceding CO_2 exposure.

Experiments with NH_4Cl

Two remarkable features of the response of pH_i in our NH_4Cl experiments are the slow acidification seen during the plateau phase (Fig. 2 B) in chronic treatments and the sizable undershoot of pH_i (Fig. 2 A) which is elicited after even brief exposures to the salt. These phenomena could be explained in several ways: the axon might respond to high values of pH_i by pumping protons inward; there may be a passive efflux of an endogenous weak base; some intracellular process could generate protons; or the NH_4^+/NH_3 couple could shuttle protons inward. None of these possibilities can presently be ruled out. However, there are a priori reasons for expecting the last to occur. Namely, NH_3 is known to be permeant, and the membrane permeability for NH_4^+ must be similar to that for K^+ in order to explain changes in V_m attending changes in $[NH_4^+]_o$ (see section entitled *Estimation of System Parameters*). It can be shown that a permeability of this magnitude is sufficient to account for the observed undershoots and the plateau phase acidifications. Thus, we feel that this simple model, which considers the simultaneous flux of both NH_4^+ and NH_3, warrants a more detailed analysis.

In this context, a graphic representation of the events taking place during and after exposure to NH_4Cl is provided by a $[NH_4^+]_i$ vs. pH_i diagram (Fig. 5 B), analogous to the graph (Fig. 5 A) discussed in connection with the CO_2 experiments. Since during the plateau phase the internal NH_3 concentration will remain essentially unchanged, and nearly identical to that in the external fluid, one may construct a background grid of "constant intracellular NH_3" curves by means of the Henderson-Hasselbalch equation applied to the equilibrium: $NH_4^+ \rightleftharpoons NH_3 + H^+$ ($pK_a' = 9.50$). Let us assume an arbitrarily low NH_3 concentration of 0.0016 mM and $pH_i = 7.30$ at the start (point A). The introduction of 10 mM NH_4^+ −ASW ($[NH_3] = 0.159$ mM) causes the system to move from A toward B. The slope of the line AB is determined by the buffering power of the intracellular fluid, while the curve BB'C represents the external NH_3 concentration, 0.159 mM. If the membrane were permeable to NH_3 only, and enough time were allowed for equilibration, then point B would characterize the new condition; conversely, removal of NH_4Cl from the medium would lead to a return, along AB, to A. However, a finite permeability to NH_4^+ (but $P_{NH_3} \gg P_{NH_4}$) leads to an influx of this ion and a reduction of the intracellular alkalinization produced by the influx of NH_3. The system's new composition would eventually be described by B', rather than by B. If the axon is returned to ASW before B' is reached (that is, before the net entry of NH_3 is complete), the system will return to curve AD'D by a path nearly parallel to AB. This is so because, due to the effect of membrane potential on ion fluxes, fewer ammonium ions will leave the axon upon removal of NH_4Cl than entered during exposure to the salt. Thus, pH_i after an exposure to NH_4Cl will be lower than that preceding exposure.

During prolonged exposures to NH_4Cl, the system not only reaches B' (indicating that internal and external NH_3 levels are nearly identical) but even moves toward C on the curve BB'C. This reduction in pH_i, which manifests itself as

a drift in the acid direction during the plateau phase, is caused by the continuing addition of protons derived from the dissociation of the entering NH_4^+, while NH_3 leaves the cell. This inward proton shuttling will continue until either one of two conditions is met: (*a*) H^+ and NH_4^+ reach Donnan equilibrium and net fluxes of both NH_3 and NH_4^+ fall to zero, or (*b*) the rate of proton pumping keeps pace with shuttling and pH_i remains constant. A steady-state scenario where shuttling by the lactic acid system in rat diaphragm muscle is balanced by proton pumping has been developed by Roos (1975). Our model predicts that pH_i should slowly fall in the plateau phase, and that, with increasing lengths of exposure to NH_4Cl, return to ASW should cause increasing amounts of undershoot. This is illustrated in Fig. 5 B, where point C represents conditions after some prolonged exposure. On removal of external NH_4Cl, point D would be reached (DC parallel to AB) if only NH_3 were permeable. If NH_4^+ is also permeable, the new condition is described by point D', slightly more alkaline than D. A further prediction is that reversal of the H^+ gradient (by depolarization, for instance) should result in a reverse shuttling and a slow alkalinization during the plateau phase.

At this point the question may be considered as to whether, and how, pH_i will ever revert to its original value after a prolonged exposure to either CO_2 or NH_4Cl. Clearly, the challenge imposed upon the cell during experiments of the type described above (intermittent exposure to relatively high levels of CO_2 and NH_4Cl) will not normally be encountered under physiological circumstances. After prolonged exposure to CO_2 or NH_4Cl, we have monitored pH_i over- and undershoots for 5–10 min after the attainment of an apparent new steady state, and have not seen any convincing evidence for a return to "normal" pH_i. However, one can envisage several mechanisms by which the axon, given more time, would eventually recover its initial pH_i value. For example, the excess protons remaining inside the axon after removal of external NH_4Cl could eventually be extruded via a H^+ pump. On the other hand, no single mechanism immediately suggests itself for replenishing the proton deficit accrued during removal of CO_2. Possibilities include (*a*) the passive influx of protons, (*b*) an inward proton pump, or (*c*) the loss of an intracellular weak base.

Experiments with Metabolic Inhibitors

The interpretation of our work with weak electrolyte metabolic inhibitors must remain uncertain, since it has not yet been possible to sort out metabolic effects from those expected from our proton shuttling model. It seems very likely that exposure of a cell to any weak acid or base can lead to significant alterations in pH_i. Therefore, due caution should be exerted when interpreting pH_i effects of metabolic inhibitors which are also weak electrolytes. Metabolic effects resulting from interference with mitochondrial activity would be expected to be in the acid direction, while changes due to proton shuttling would be in the direction determined by the H^+ electrochemical gradient.

Estimation of System Parameters

As indicated in the Appendix, our model can be used to select such values for

the parameters: buffering power, permeabilities, and proton pumping rates, as will yield a theoretical curve which fits the observed one. Rapid changes in pH_i produced by azide, CO_2, and NH_4^+ require a buffering power β (see Eq. 6 of the Appendix for definition) in the range −9 to −33 mM. These estimates are not inconsistent with the values for β extracted from Spyropoulos' (1960) titration of extruded squid axoplasm, which extend from −14 to −52 mM over the pH range 6–8. Although we have treated β as a constant in our preliminary calculations, variations with pH_i would be compatible with our results, and would not affect the qualitative aspects of our argument.

The permeability of the membrane to NH_4^+ should be the major factor in determining the rate of proton shuttling during the plateau phase. From the relative effect on V_m of increasing by 10 mM either external NH_4^+ or K^+ concentrations in ASW (see page 97) we estimate that P_{NH_4} is of the same order of magnitude as P_K. If K^+ influx is normally about 50 pmol/cm²s (Caldwell and Keynes, 1960), then the constant field assumption leads to a P_K of about 6.7×10^{-8} cm/s. Thus, P_{NH_4} may be about 6×10^{-8} cm/s. A similar value for P_{NH_4}, when employed in the mathematical model, leads to a predicted proton shuttling rate close to that actually observed in our long-term NH_4^+ experiments.

Attempts to estimate the permeability of the membrane to NH_3 and especially to CO_2 are complicated by the 9-s time constant of the recording apparatus. Furthermore, the uncatalyzed hydration reaction: $CO_2 + H_2O \rightarrow H_2CO_3$ has a time constant of about 27 s at 25°C (Edsall and Wyman, 1958). Thus, in the absence of carbonic anhydrase, intracellular acidification resulting from the influx of CO_2 can be expected to be a rather slow process. It follows that it will be difficult to distinguish between the absence of carbonic anhydrase and a low permeability to CO_2 as causes for the relatively slow (1–2 min) fall in pH_i at the onset of an exposure to CO_2. Consequently, in our mathematical treatment of the data (see Appendix), we have lumped permeation and hydration of CO_2 into a single event governed by a parameter conveniently termed "permeability."

Proton pumping rates needed to explain our data on both short- and long-term CO_2 exposures cannot be estimated without defining the parameters that determine the H^+ pumping rate. If the total rate at which protons are pumped is given by $k[H^+]_i$, where k is a rate constant, and the rate at which protons are pumped during the control period is $k[H^+]_i'$ then we define the rate of additional proton pumping in response to an intracellular acid load (M_H) by

$$M_H = k([H^+] - [H^+]').$$

Here we have assumed that the background rate of passive proton influx (and thus the background proton pumping rate $k[H^+]'$) during experimental conditions is identical to the total acid flux (and to the total pumping rate) during control conditions. Our data indicate that k is at least 75 s^{-1}.

APPENDIX

Kinetics of Intracellular pH Changes upon Exposure to Weak Acids or Bases

In this section we derive the differential equations for the *time-course* of pH_i as determined

by the intracellular buffering power and by the "proton load" (positive or negative) imposed upon the cell after exposure to a weak acid. Similar equations can also be derived for the case of a weak base.

Derivation

We assume Fick's law to govern the net passive flux of uncharged particles, and the constant field equation (Goldman, 1943; Hodgkin and Katz, 1949) to describe that of charged species:

$$M_{HA} = P_{HA}([HA]_o - [HA]_i), \tag{1 a}$$

$$M_A = \frac{P_A V_m F}{RT} \cdot \frac{[A]_o - [A]_i \epsilon}{1 - \epsilon}, \tag{2 a}$$

where M_{HA} and M_A represent the net inward fluxes of the weak acid and conjugate base, respectively; P_{HA} and P_A are permeabilities; the subscripts i and o refer to internal and external concentrations, respectively; V_m is the membrane potential; ϵ represents $\exp(-V_m F/RT)$; and F, R, and T have their usual meaning. These two fluxes, and the area/volume ratio of the cell (ρ), determine the time rate of change of total intracellular weak acid concentration ($[TA]_i$):

$$\frac{d[TA]_i}{dt} = (M_{HA} + M_A)\,\rho. \tag{3 a}$$

A fraction (α) of the total intracellular weak acid remains undissociated:

$$\alpha = \frac{[HA]_i}{[HA]_i + [A]_i} = \frac{[H]_i}{[H]_i + K}, \tag{4 a}$$

where K is the acid dissociation constant. Thus, a fraction (α) of the entering A^- will combine with H^+, and a portion ($1 - \alpha$) of the entering HA will dissociate into $A^- + H^+$. The proton load imposed upon the cell interior is then determined by (*a*) the production of protons from entering HA, or $(1 - \alpha)M_{HA}$, and (*b*) their consumption by entering A^-, or αM_A. Consequently, if dQ/dt represents the rate at which protons are added to the cell per unit volume, we have

$$\frac{dQ}{dt} = \rho\,[(1 - \alpha)M_{HA} - \alpha M_A - M_H], \tag{5 a}$$

where the additional term M_H represents the rate (in mol cm^{-2} s^{-1}) of intracellular consumption and/or active extrusion of protons in excess of that occurring in the control state.

The time rate of changes of the *free* proton concentration is a function of intracellular buffering power, classically defined as $\beta = dQ/dpH$. Since 2.303 pH = ln $[H]_i$, or 2.303 dpH = $-d[H]_i/[H]_i$, we have

$$\frac{d[H]_i}{dt} = \frac{-2.303\,[H]_i}{\beta} \cdot dQ, \tag{6 a}$$

and, combining Eqs. 5 *a* and 6 *a*,

$$\frac{d[H]_i}{dt} = \frac{-2.303\,[H]_i \rho}{\beta}[(1 - \alpha)M_{HA} - \alpha M_A - M_H]. \tag{7 a}$$

Substitution of $[HA]_i = \alpha[TA]_i$ and $[A]_i = (1 - \alpha)[TA]_i$ into Eqs. 3 *a* and 7 *a* yields the desired set of differential equations in terms of $[TA]_i$ and $[H]_i$:

$$\frac{d[TA]_i}{dt} = \rho \left[P_{HA}([HA]_o - \frac{[H]_i}{[H]_i + K}[TA]_i) + \frac{P_A V_m F}{RT} \cdot \frac{[A]_o - \frac{K}{[H]_i + K}[TA]_i\epsilon}{1 - \epsilon} \right] \quad (8\,a)$$

$$\frac{d[H]_i}{dt} = \frac{-2.303\,[H]_i\rho}{\beta} \left[\frac{K}{[H]_i + K} P_{HA}([HA]_o - \frac{[H]_i}{[H]_i + K}[TA]_i) - \frac{[H]_i}{[H]_i + K} \cdot \frac{P_A V_m F}{RT} \cdot \frac{[A]_o - \frac{K}{[H]_i + K}[TA]_i\epsilon}{1 - \epsilon} - M_H \right]. \quad (9\,a)$$

These simultaneous equations, which have no general analytical solution, were solved numerically by computer. (The time-course of the concentrations of HA and A^- individually can be computed from $[H]_i$, $[TA]_i$, and K.) Fig. 6 A illustrates the result of such computations applied to a typical CO_2 experiment. By systematically altering the various parameters, the mathematical model can be made to fit the experimental results: the *initial rate* of pH decrease is approximately proportional to the permeability of the membrane to CO_2; the *extent* of this initial change is nearly proportional to the buffering power; and the rate of pH change during the *plateau phase* is determined by the extent to which proton pumping exceeds proton entry via the CO_2/HCO_3^- shuttle. Obviously, a lower limit for the rate of additional H^+ pumping is obtained in the case where the permeability to HCO_3^- is put equal to zero.

Weak Base

An analogous derivation for the case of a weak base ($BH^+ \rightleftarrows B + H^+$) leads to the following equations:

$$\frac{d[TB]_i}{dt} = \rho \left[P_B([B]_o - \frac{K}{[H]_i + K}[TB]_i) + \frac{P_{HB} V_m F}{RT} \cdot \frac{[HB]_o - \frac{[H]_i}{[H]_i + K}[TB]_i\epsilon'}{\epsilon' - 1} \right], \quad (10\,a)$$

$$\frac{d[H]_i}{dt} = \frac{-2.303\,[H]_i\rho}{\beta} \left[\frac{K}{[H]_i + K} \cdot \frac{P_{HB} V_m F}{RT} \cdot \frac{[HB]_o - \frac{[H]_i}{[H]_i + K}[TB]_i\epsilon'}{\epsilon' - 1} - \frac{[H]_i}{[H]_i + K} P_B([B]_o - \frac{K}{[H]_i + K}[TB]_i) - M_H \right], \quad (11\,a)$$

where $[TB]_i$ is the intracellular concentration of total base, P_{HB} and P_B are permeabilities, and $\epsilon' = \exp(V_m F/RT)$. Fig. 6 B illustrates typical examples of the numerical solutions to Eqs. 10 *a* and 11 *a* for the case of exposure to NH_4Cl. Again, certain aspects of the pH_i time-course are primarily affected by specific parameters: the initial rate of pH_i increase

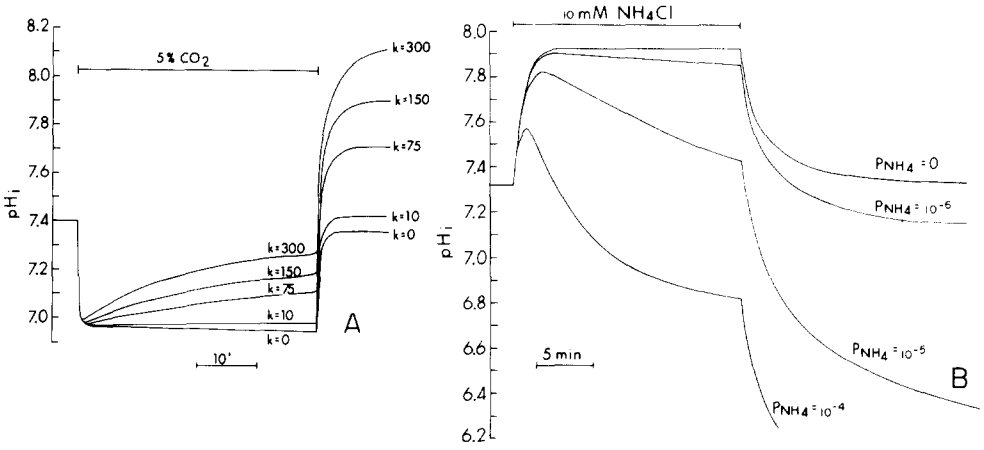

FIGURE 6. (A) Computer-simulated pH_i time-course during and after exposure to CO_2. Variations in k, the proton pump rate constant (given in s^{-1}), result in changes in the plateau phase slope and the amount of overshoot. When $k = 0$ (no pumping) pH_i actually declines in the plateau phase and falls short of the initial pH_i upon removal of the CO_2. In these plots, $pK_a' = 6.00$, $\beta = -26$ mM, $P_{HCO_3} = 5 \times 10^{-7}$ cm/s, $p_{CO_2} = 6 \times 10^{-3}$ cm/s, $pH_o = 7.70$, $p_{CO_2} = 37$ mm Hg (5% CO_2), $T = 23°$, and fiber diameter = 500 μm. (B) Computer-simulated pH_i time-course during and after exposure to NH_4Cl. Variations of P_{NH_4}, the permeability of the membrane to NH_4^+ (given in centimeters per second), produce changes in the plateau phase slope and the amount of undershoot. When $P_{NH_4} = 0$, the plateau phase is nearly horizontal, and pH_i returns to exactly the initial pH_i after removal of external NH_4Cl. When P_{NH_4} is very large proton shuttling takes place at a very rapid pace, and pH_i soon approaches the value predicted from Donnan theory. In these plots, $pK_a' = 9.50$, $\beta = -9$ mM, $P_{NH_3} = 6 \times 10^{-3}$ cm/s, $[NH_4Cl]_o = 10$ mM, $pH_o = 7.70$, k (H^+ pump rate constant) = 0, $T = 23°$, and fiber diameter = 500 μm.

is determined mainly by P_{NH_3}, the extent of the initial change in pH_i by β, and the slope of the plateau phase by P_{NH_4}.

Special Case: Constant pH_i

Consider the case of Eqs. 8 *a* and 9 *a* in which $d[H]_i/dt = 0$. This condition is met by assuming either an infinite buffering power ($\beta \to -\infty$) or, more realistically, a rate of proton extrusion equal to the rate at which protons are carried into the cell by the HA/A^- shuttle. Note that constant pH_i does not necessarily imply a steady state with respect to the other variables. The analytical solution to the remaining equation (8 *a*) is readily obtained and describes the time-course of total intracellular acid concentration:

$$[TA]_i = \frac{P_{HA}[HA]_o + \dfrac{P_A V_m F [A]_o}{RT(1-\epsilon)}}{P_{HA} \cdot \dfrac{[H]_i}{[H]_i + K} + \dfrac{P_A V_m F \epsilon}{RT(1-\epsilon)} \cdot \dfrac{K}{[H]_i + K}} \cdot \left[1 - \exp\left[-t \cdot \rho\left(P_{HA} \cdot \frac{[H]_i}{[H]_i + K} + \frac{P_A V_m F \epsilon}{RT(1-\epsilon)} \cdot \frac{K}{[H]_i + K}\right)\right]\right]. \quad (12\ a)$$

At infinite time, $[TA]_i$ reaches a constant value. If $[TA]_i$ ($t = \infty$) is substituted into Eqs. 1 *a* and 2 *a*, $M_{HA} = -M_A$. This special case is essentially a restatement of the equation developed by Roos (1965) for the steady-state distribution of a weak acid across a cell membrane.

We are indebted to M. P. Blaustein, E. L. Boulpaep, B. G. Kennedy, and C. M. Rovainen for critical comments on an earlier draft of this paper and especially to A. Roos for many helpful discussions during the course of this work. One of us (W. F. B.) is grateful to J. A. M. Hinke in whose laboratory the technique for fabricating pH_i electrodes was learned. We thank E. Y. Rodin for verifying the mathematics, and thank the Director of the Marine Biological Laboratory, Woods Hole, Massachusetts for facilities placed at our disposal. The expert assistance of V. Creasy in the construction of the horizontal chamber, of G. Jerman in preparing the manuscript, and of S. McConnell with some of the drawings, is gratefully acknowledged.

Supported by a fellowship from the Grass Foundation (to W. F. B.), and by NIH Grants NS 11223 (to P. D. W.) and HL 00082 (to A. Roos). Boron is supported by Medical Scientist Training Program Fellowship, GM 02016.

Received for publication 10 March 1975.

REFERENCES

BATES, R. G. 1973. Determination of pH. Theory and Practice. John Wiley & Sons, New York.

BICHER, H., and S. OHKI. 1972. Intracellular pH electrode experiments on the giant squid axon. *Biochim. Biophys. Acta.* **255**:900.

BORON, W. F., and P. DE WEER. 1975. Studies on the intracellular pH of squid giant axons. *Biophys. J.* **15**:42a.

BRINLEY, F. J., JR., and L. J. MULLINS. 1967. Sodium extrusion by internally dialyzed squid axons. *J. Gen. Physiol.* **50**:2303.

CALDWELL, P. C. 1954. An investigation of the intracellular pH of crab musle fibres by means of micro-glass and micro-tungsten electrodes. *J. Physiol. (Lond.).* **126**:169.

CALDWELL, P. C. 1958. Studies on the internal pH of large muscle and nerve fibres. *J. Physiol. (Lond.).* **142**:22.

CALDWELL, P. C., and R. D. KEYNES. 1960. The permeability of the squid giant axon to radioactive potassium and chloride ions. *J. Physiol. (Lond.).* **154**:177.

CARTER, N. W., F. C. RECTOR, JR., D. S. CAMPION, and D. W. SELDIN. 1967. Measurement of intracellular pH of skeletal muscle with pH-sensitive glass microelectrodes. *J. Clin. Invest.* **46**:920.

COLE, K. S., and J. W. MOORE. 1960. Liquid junction and membrane potentials of the squid giant axon. *J. Gen. Physiol.* **43**:971.

DE WEER, P., and D. GEDULDIG. 1975. Effect of cyanide on the resting membrane potential of squid giant axon. *Biophys. J.* **15**:42a.

DONNAN, F. G. 1924. The theory of membrane equilibria. *Chem. Rev.* **1**:73.

EDSALL, J. T., and J. WYMAN. 1958. Biophysical Chemistry, Vol. I. Academic Press, Inc., New York.

GOLDMAN, D. 1943. Potential, impedance and rectification in membranes. *J. Gen. Physiol.* **27**:37.

HARNED, H. S., and F. T. BONNER. 1945. The first ionization of carbonic acid in aqueous solutions of sodium chloride. *J. Am. Chem. Soc.* **67**:1026.

HARNED, H. S., and R. DAVIS, JR. 1943. The ionization constant of carbonic acid in water

and the solubility of carbon dioxide in water and aqueous salt solutions from 0 to 50°. *J. Am. Chem. Soc.* **65**:2030.

HINKE, J. A. M. 1967. Cation-selective microelectrodes for intracellular use. *In* Glass Electrodes for Hydrogen and Other Cations. G. Eisenman, editor. Marcel Dekker, New York. 464.

HODGKIN, A. L., and KATZ, B. 1949. The effect of sodium ions on the electrical activity of the giant axon of the squid. *J. Physiol. (Lond.).* **108**:37.

HOWELL, B. J., F. W. BAUMGARDNER, K. BONDI, and H. RAHN. 1970. Acid-base balance in cold-blooded vertebrates as a function of body temperature. *Am. J. Physiol.* **218**:600.

JACOBS, M. H. 1940. Some aspects of cell permeability to weak electrolytes. *Cold Spring Harbor Symp. Quant. Biol.* **8**:30.

KOSTYUK, P. G., Z. A. SOROKINA, and Y. D. KHOLODOVA. 1969. Measurement of activity of hydrogen, potassium, and sodium ions in striated muscle fibers and nerve cells. *In* Glass Microelectrodes. M. Lavallée, O. F. Schanne, and N. C. Hébert, editors. John Wiley & Sons, Inc., New York. 322.

MCLAUGHLIN, S. G. A., and J. A. M. HINKE. 1968. Optical density changes of single muscle fibers in sodium-free solutions. *Can. J. Physiol. Pharmacol.* **46**:247.

MITCHELL, P. 1961. Conduction of protons through the membranes of mitochondria and bacteria by uncouplers of oxidative phosphorylation. *Biochem. J.* **81**:248.

ORLOFF, J., and R. W. BERLINER. 1956. The mechanism of the excretion of ammonia in the dog. *J. Clin. Invest.* **35**:223.

PAILLARD, M. 1972. Direct intracellular pH measurement in rat and crab muscle. *J. Physiol. (Lond.).* **223**:297.

REEVES, R. B. 1972. An imidazole alphastat hypothesis for vertebrate acid-base regulation: tissue carbon dioxide content and body temperature in bull frogs. *Respir. Physiol.* **14**:219.

ROOS, A. 1965. Intracellular pH and intracellular buffering power of the cat brain. *Am. J. Physiol.* **209**:1233.

ROOS, A. 1971. Intracellular pH and buffering power of rat muscle. *Am. J. Physiol.* **221**:182.

ROOS, A. 1975. Intracellular pH and distribution of weak acids across cell membranes. A study of D- and L-lactate and of DMO in rat diaphragm. *J. Physiol. (Lond.).* **249**:1.

SPYROPOULOS, C. S. 1960. Cytoplasmic pH of nerve fibres. *J. Neurochem.* **5**:185.

THOMAS, R. C. 1974 *a*. Intracellular pH of snail neurones measured with a new pH-sensitive glass microelectrode. *J. Physiol. (Lond.).* **238**:159.

THOMAS, R. C. 1974 *b*. The effect of bicarbonate on the intracellular buffering power of snail neurones. *J. Physiol. (Lond.).* **241**:103P.